Article

Biogeographic response of marine plankton to Cenozoic environmental changes

https://doi.org/10.1038/s41586-024-07337-9

Received: 2 May 2023

Accepted: 20 March 2024

Published online: 17 April 2024

Check for updates

Anshuman Swain[1,2,3,4,8]✉, Adam Woodhouse[5,6,8], William F. Fagan[4], Andrew J. Fraass[7] & Christopher M. Lowery[5]

In palaeontological studies, groups with consistent ecological and morphological traits across a clade's history (functional groups)[1] afford different perspectives on biodiversity dynamics than do species and genera[2,3], which are evolutionarily ephemeral. Here we analyse Triton, a global dataset of Cenozoic macroperforate planktonic foraminiferal occurrences[4], to contextualize changes in latitudinal equitability gradients[1], functional diversity, palaeolatitudinal specialization and community equitability. We identify: global morphological communities becoming less specialized preceding the richness increase after the Cretaceous–Palaeogene extinction; ecological specialization during the Early Eocene Climatic Optimum, suggesting inhibitive equatorial temperatures during the peak of the Cenozoic hothouse; increased specialization due to circulation changes across the Eocene–Oligocene transition, preceding the loss of morphological diversity; changes in morphological specialization and richness about 19 million years ago, coeval with pelagic shark extinctions[5]; delayed onset of changing functional group richness and specialization between hemispheres during the mid-Miocene plankton diversification. The detailed nature of the Triton dataset permits a unique spatiotemporal view of Cenozoic pelagic macroevolution, in which global biogeographic responses of functional communities and richness are decoupled during Cenozoic climate events. The global response of functional groups to similar abiotic selection pressures may depend on the background climatic state (greenhouse or icehouse) to which a group is adapted.

Geographic range shifts due to ongoing climate change fundamentally alter community structure and function[6,7]. Growing evidence demonstrates that the latitudinal biodiversity gradient (LBG) is not static over geological time, reflecting adaptive biological and phylogenetic responses to environmental change[2,8–12]. Determining the mechanistic drivers of ancient and modern biogeography is core to understanding how biodiversity operates as a whole, and ultimately adapts to environmental changes over varying geological and anthropogenic timescales[8].

Unlike terrestrial LBGs, which peak at the Equator, modern marine LBGs peak within the tropics, with a slight richness reduction at the Equator[2,8,9,13]. The vast distances and complex oceanography of the modern marine domain create distinct biogeographic provinces that depend in part on latitude, temperatures, ocean currents and other factors[9], facilitating geographical and bathymetric restriction of gene flow between populations, strengthening pelagic LBGs[2].

Fenton et al.[2] used the unparalleled fossil record of the planktonic foraminifera to demonstrate that the modern marine LBG was probably established about 15 Myr ago (Ma), before which fundamentally different biodiversity distributions were in place. Concurrently, Woodhouse, Swain et al.[1] documented the presence of a latitudinal equitability gradient (LEG; which measures how equitable distributions are of species or functional groups) among the planktonic foraminifera, based on the functional groupings of ecological and morphological traits (hereafter ecogroups and morphogroups, respectively) assigned by Aze et al.[14] (Fig. 1). In the modern ocean, the LEG closely matches the LBG among planktonic foraminifera[1], wherein spatial diversity patterns also correspond with those of many marine resources fundamental to humanity[15]. However, before 2 Ma, the planktonic foraminiferal LEG was independent from the LBG. This observation may have direct consequences on these resources as anthropogenic climate change continues. Past work has used similar metrics at a coarser temporal resolution for Bivalvia, a model macrofossil group, and demonstrated a correlation between taxonomic and functional diversity in the modern, but temporal decouplings between diversity measures during two major mass extinction events (Cretaceous/Palaeogene (K/Pg) and Permo/Triassic)[16].

At present, there is no spatiotemporal documentation of the relationship between LBGs and LEGs before 15 Ma, during ancient intervals that may represent analogues to potential future climates[17]. Studies prospecting geological intervals before the initiation of the icehouse

[1]Department of Organismic and Evolutionary Biology, Harvard University, Cambridge, MA, USA. [2]Museum of Comparative Zoology, Harvard University, Cambridge, MA, USA. [3]Department of Paleobiology, National Museum of Natural History, Washington, DC, USA. [4]Department of Biology, University of Maryland, College Park, MD, USA. [5]University of Texas Institute for Geophysics, University of Texas at Austin, Austin, TX, USA. [6]School of Earth Sciences, University of Bristol, Bristol, UK. [7]School of Earth and Ocean Sciences, University of Victoria, Victoria, British Columbia, Canada. [8]These authors contributed equally: Anshuman Swain, Adam Woodhouse. ✉e-mail: anshumanswain@fas.harvard.edu

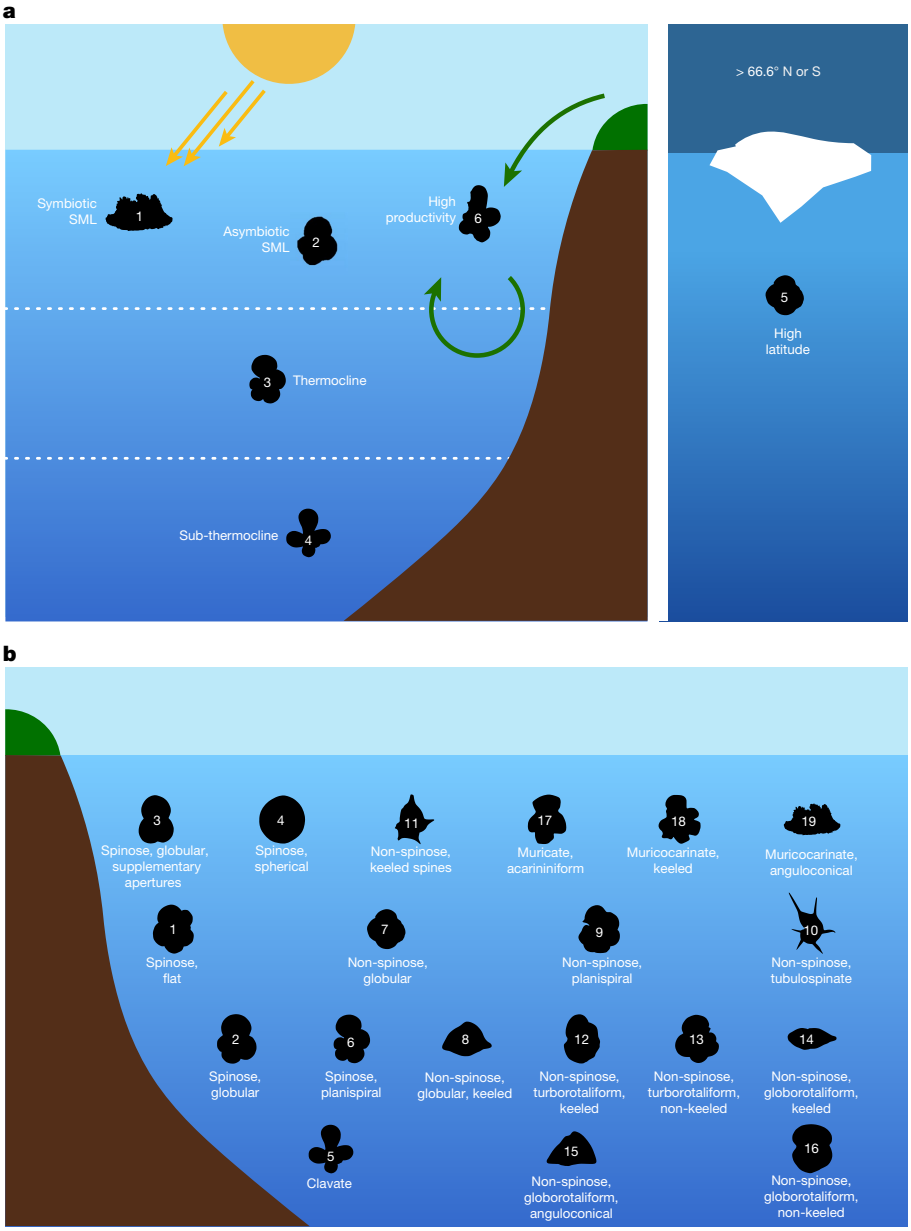

Fig. 1 | Foraminiferal functional groups. a,**b**, Representation of planktonic foraminiferal ecogroups (**a**) and morphogroups (**b**) of ref. 14 with updates from ref. 28. Ecogroups are based on inferred ecology from geochemical, biogeographic and taxonomic studies, and morphogroups are based on external test morphology[14]. For ecogroups: (1) open ocean surface mixed layer (SML) dwellers with algal photosymbionts, (2) open ocean surface mixed layer dwellers without algal photosymbionts, (3) open ocean thermocline dwellers, (4) open ocean sub-thermocline dwellers, (5) high-latitude dwellers, (6) high-productivity- or upwelling-region dwellers. For morphogroups, position in the water column is approximate for each represented morphogroup member, and may not be consistent across morphogroups. Diagram in **a** adapted from ref. 1, Springer Nature Limited; silhouettes in **a**,**b**, adapted with permission from Brian Huber and Jeremy Young.

climate regime at the Eocene–Oligocene transition (EOT, about 34 Ma) suggest that life may have exhibited extratropical LBG peaks in response to higher global temperatures[11]. A fundamental palaeoceanographic change occurred at the EOT, as a global reorganization of ocean circulation and strengthening of the biological carbon pump had important consequences for LBGs across this interval (for example, refs. 10,18). However, these previous works focused on specific time intervals, and were built from small numbers of individual sites. No complete record of marine biodiversity change with a focus on LEGs, functional richness and community dynamics exists for the Cenozoic era as a whole.

Here we build on our previous analyses of functional community and LEG responses of planktonic foraminifera to climatic perturbations over the late Neogene[1] by extending them from a 15-Myr period to the entire 66-Myr Cenozoic, which allows us to analyse a much broader range of climate states and the mass extinction events at the K/Pg boundary and EOT. Applying methods from network science[1] to Triton, a global dataset of Cenozoic macroperforate planktonic foraminiferal records with >500,000 individual species occurrences[4], we delineate spatiotemporal changes in foraminiferal functional group diversity and community structure using the ecogroup and morphogroup framework of Aze et al.[14]. Specifically, we use bipartite network representations, which feature two classes of nodes and links that can exist only between nodes of different classes (in our case, ecogroups and morphogroups as one class and 5° palaeolatitudinal bands as the other), to capture the complex interconnected nature of ecogroup and morphogroup biogeographical co-occurrences in a holistic and

new way. We build such networks for every 1-Myr temporal bin for the whole Cenozoic, for which the width of the links between a functional group and a palaeolatitudinal band denotes the number of occurrences of that group at that particular palaeolatitudinal band in each given temporal bin (Methods).

After ensuring requisite sampling completeness in our data (sample coverage; Extended Data Figs. 1 and 2), we explored patterns in the biogeographical distribution of ecogroups and morphogroups (Fig. 1) during the Cenozoic through network metrics. In particular, we considered the following metrics: the richness (that is, number) of ecogroups or morphogroups in each palaeolatitudinal band (that is, degree for each palaeolatitudinal band node); the ecogroup and morphogroup specialization index (ESI and MSI); and the ecogroup and morphogroup paired difference index. Specialization and paired difference indices measure, in slightly different ways, how equitable the distribution of ecogroups and morphogroups is in a given palaeolatitudinal band in reference to all other palaeolatitudinal bands within each discrete 1-Myr temporal bin. Lower values within these metrics (denoted by warmer colours) indicate higher equitability among these groups (that is, a palaeolatitudinal band having an equal number of occurrences of all functional groups of interest will have low values of ESI or MSI and one having only a dominant group will have high values; see ref. 1 and Methods for further details).

We plotted these metrics alongside Cenozoic stable isotopic benthic oxygen ($\delta^{18}O$) and carbon ($\delta^{13}C$) data from Westerhold et al.[19] to assess changes through the lens of Cenozoic climate change (Figs. 2 and 3 and Extended Data Fig. 3; see Extended Data Fig. 4 for Shannon diversity measures for species, ecogroups and morphogroups for comparison). For each temporal bin, we then fitted logistic regressions to the global richness and specialization indices and calculated the logistic inflection point, which denotes the maximum rate of change during each discrete study interval. This inflection point is usually the midpoint of richness and specialization index transitions, and not the point where the transition starts or finishes (see Methods for details on the fit). Furthermore, it should be noted that even although all statistical analyses of our work were checked for robustness, they assume that the underlying data are equally robust as well; therefore, we suggest caution in interpreting results for which data are sparse (for example, the early Palaeocene) and encourage future work into specific intervals in Triton for which there are data deficiencies at present.

We identify five shifts among functional richness and LEGs with major implications for understanding how Cenozoic palaeoclimate affected macroevolution among plankton ecosystems: a substantial shift to more generalized global morphological communities about 4 Myr following the K/Pg mass extinction (about 66 Ma); southern high-latitude refugia for generalized ecological communities facilitating a unimodal LEG during the peak warmth of the Cenozoic greenhouse (about 56–49 Ma), which was otherwise characterized by cosmopolitan specialized ecological communities; a shift to morphologically specialized communities about 2 Myr before the marked loss of morphological diversity at the EOT (about 34 Ma) and a unimodal LEG through the entire Oligocene; a synchronous shift in both morphological specialization and richness in the early Miocene (about 19 Ma), coeval with a recently identified extinction in pelagic sharks[5]; and a hemisphere-wide delay between functional group exploitation of new niches during the mid-Miocene diversification of calcareous plankton (about 15 Ma). Our analyses shine a light on new patterns in Cenozoic pelagic biogeography, and provide a quantitative, palaeobiogeographic underpinning to a variety of previously established hypotheses on global marine biodiversity response to Cenozoic climate change.

Recovery in post-K/Pg morphogroups

Background extinctions, as well as the 'Big Five' mass extinction events, are followed by an approximately 10-Myr delay in peak origination rates[20–22]. This delay is thought to be caused by the gradual reconstruction of morphospace that needs to be developed before it can be filled out[20], a hypothesis supported by data for planktonic foraminifera following the K/Pg mass extinction event (66 Ma)[21]. Our results show that a substantial increase in global macroperforate planktonic foraminiferal morphogroup richness exhibits an approximately 5-Myr delay following the K/Pg event (Fig. 3b and Extended Data Fig. 5a) in agreement with results for all planktonic foraminiferal morphological complexity[21]. However, our calculated logistic inflection indicates that richness of macroperforates increased most quickly about 62 Ma (61.72; $P < 10^{-6}$; Extended Data Fig. 5a), leading to a new stabilized value of richness of this group by about 60 Ma.

However, MSI values, (which indicate a significant, rapid reduction in specialization among the macroperforates about 3 Myr (logistic inflection at 62.9 ± 1.6 Ma $P < 0.05$)) after the K/Pg event, preceded the rapid rise in richness values by about 1 Myr (logistic inflection at 61.7 ± 0.34 Ma; Fig. 3c and Extended Data Fig. 5b; Methods) after the event. This shift away from specialized morphological communities occurs following the increase in efficiency of the marine biological carbon pump (about 1.8 Myr[23,24]), the re-establishment of marine community equilibria and food webs (about 1.8 Myr[25,26]), increased water column oligotrophy (about 2.0 Myr[18]) and the reacquisition of photosymbiosis within planktonic foraminifera (about 2.3 Myr[24,27]). Unlike many of the later events we document through the Cenozoic, there seems to be no discernible pattern within the spatial dynamics of this observation. The shift to more generalized morphological communities about 63 Ma approximates the time at which three major photosymbiotic foraminiferal clades rose to importance during the Palaeogene: *Igorina, Morozovella* and *Acarinina*[4]. All three clades exhibited the presence of algal symbionts; however, the last two expressed a morphologically distinct 'muricate' wall texture, recently proven to have housed spines[28]. Spines, alongside the presence of algal symbionts, were adaptations that probably allowed these taxa to fill out new ecological niches in the newly oligotrophic habitats of the upper ocean following the restoration of the biological pump[18,29]. Although spines represent a pioneering ecological innovation, they seem to have had no discernible effect on ecogroup community metrics at this time (Fig. 2b). This may indicate that: the distinct establishment of more generalized morphological communities at about 63 Ma (Fig. 3b and Extended Data Fig. 5b) occurred within already equitable ecogroup communities; or the inception of photosymbiosis among the Cenozoic macroperforate planktonic foraminifera, possibly within southern high palaeolatitudes, was followed by a delayed radiation among certain muricate groups[30].

Furthermore, the three morphogroups present that stemmed from survivors of the K/Pg extinction before the evolution of muricate taxa (spinose, globular; non-spinose, globular; and non-spinose, turborotaliform, non-keeled[14]; Fig. 1) were already well established within the first approximately 200 kyr of the Cenozoic, yet it was not until the evolution of muricate spine-bearers and 'full' planktonic biotic recovery (about 4.3 Myr[24]) that a substantial increase in diversification took place, primarily and synchronously among symbiont-bearing mixed layer and thermocline dwellers[31,32]. This observation suggests that irrespective of the phylogenetic longevity of these morphologies, once the physicochemical state of the ocean and efficiency of the biological pump had returned to its pre-K/Pg state after about 1.8–2 Myr[23–26], all macroperforate morphologies required the same duration of time to become equitably distributed (about 3 Myr; Fig. 3c), and then to regain their morphological complexity (about 5 Myr[21]).

Additionally, patterns of consistently heightened morphogroup specialization indices within post-K/Pg southern high palaeolatitudes (Fig. 3c and Extended Data Fig. 3b) accord with observations of greater planktonic foraminiferal endemism across this region during the early Palaeocene[33]. Specifically, for the first 3 Myr of the Cenozoic, we find that the MSI of palaeolatitudes 50–65° S differs from that of all other palaeolatitudes ($P < 0.05$, one-tailed t-test). At present, it is not possible

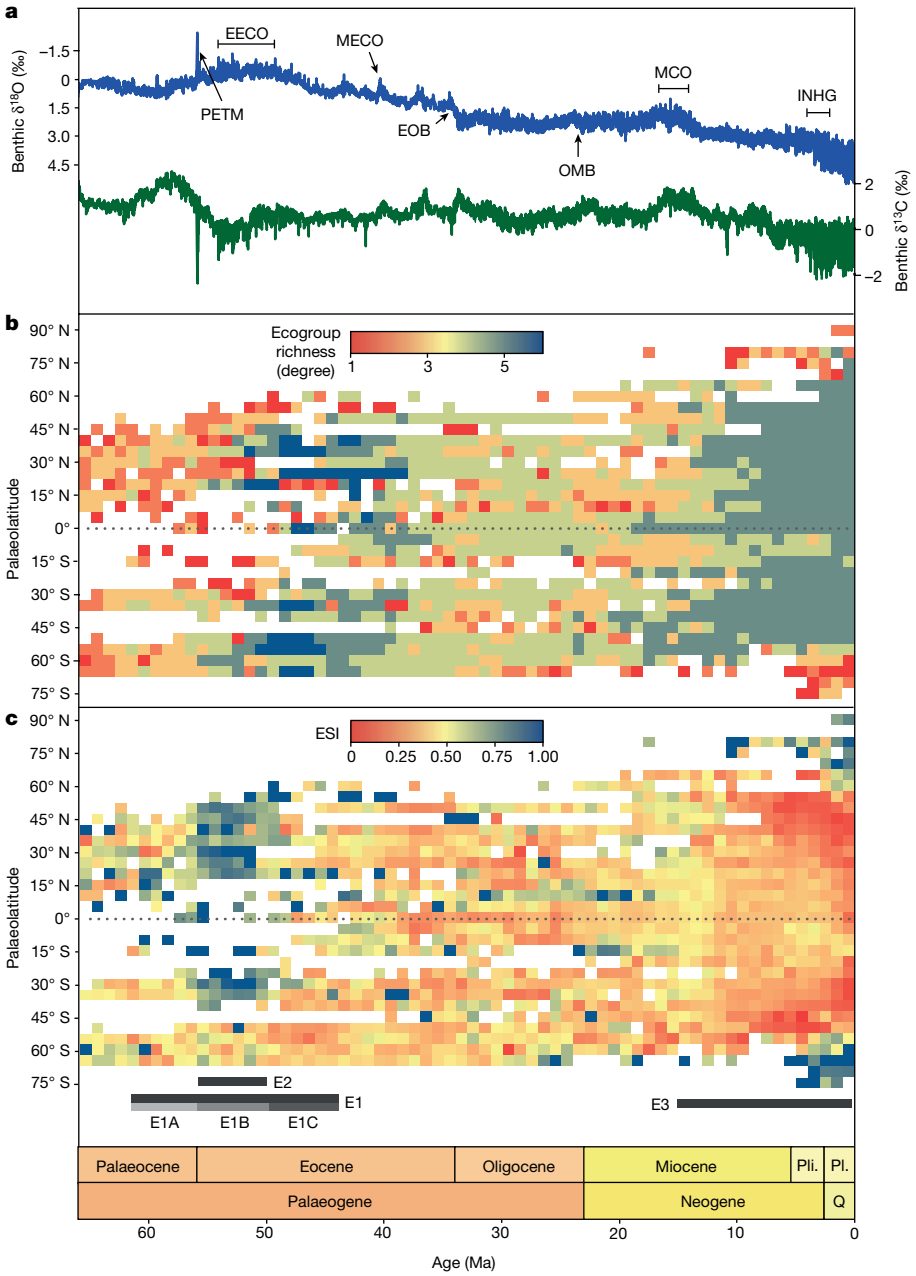

Fig. 2 | Cenozoic climate and ecogroup metrics. a, Benthic $\delta^{18}O$ and $\delta^{13}C$ from ref. 19. PETM, Palaeocene–Eocene Thermal Maximum; MECO, Middle Eocene Climatic Optimum; EOB, Eocene–Oligocene boundary; OMB, Oligocene–Miocene boundary; MCO, Miocene Climatic Optimum; INHG, Intensification of Northern Hemisphere Glaciation. **b**, Ecogroup richness (degree or number of ecogroups). **c**, ESI. Note that in **b**,**c** the Northern Hemisphere bands extend to 90° N whereas the Southern Hemisphere bands extend to 75° S. Blue colours equal high ecogroup richness (**b**) or specialization (**c**), whereas red colours correspond to low values of each metric. The events of interest are noted in **c**—E1: sustained higher ecogroup specialization across all latitudes during the interval E1B (56–50 Ma) than during either the preceding E1A (62–56 Ma) or succeeding E1C (50–44 Ma) intervals; E2: extreme low Southern Hemisphere mid–high-latitude ecogroup specialization values (56–50 Ma); E3: a significant delay between niche exploitation and diversification as bipolar ice sheet expansion triggered global paleoceanographic change. Pli, Pliocene; Pl., Pleistocene; Q, Quaternary.

to determine whether the same pattern is reflected within the Northern Hemisphere high latitudes or whether low latitudes were warm enough to hinder hemispheric dispersion owing to the lack of these spatial records in Triton (and the palaeontological record more broadly[2,4,12]; Figs. 2 and 3). However, the occurrence of endemic circum-Antarctic faunas[33] as well as the evolution of photosymbiosis in southern high palaeolatitudes[30] suggests that polar currents may have promoted vicariance among marine plankton populations under the influence of warm high-latitude temperatures suggested during the early Cenozoic greenhouse[34].

Refugia in Early Eocene Climatic Optimum ecogroups

Ecogroup specialization indices (Fig. 2c and Extended Data Fig. 3c) increased globally at the initiation of the Palaeocene–Eocene Thermal Maximum (about 56 Ma), and remained high until the termination of the Early Eocene Climatic Optimum (EECO; about 53.3–49.1 Ma), the peak period of sustained warmth during the Cenozoic[19]. Studies have suggested that poleward extirpation from lower latitudes during the height of the Palaeocene–Eocene Thermal Maximum—the most extreme and geologically rapid warming event of the

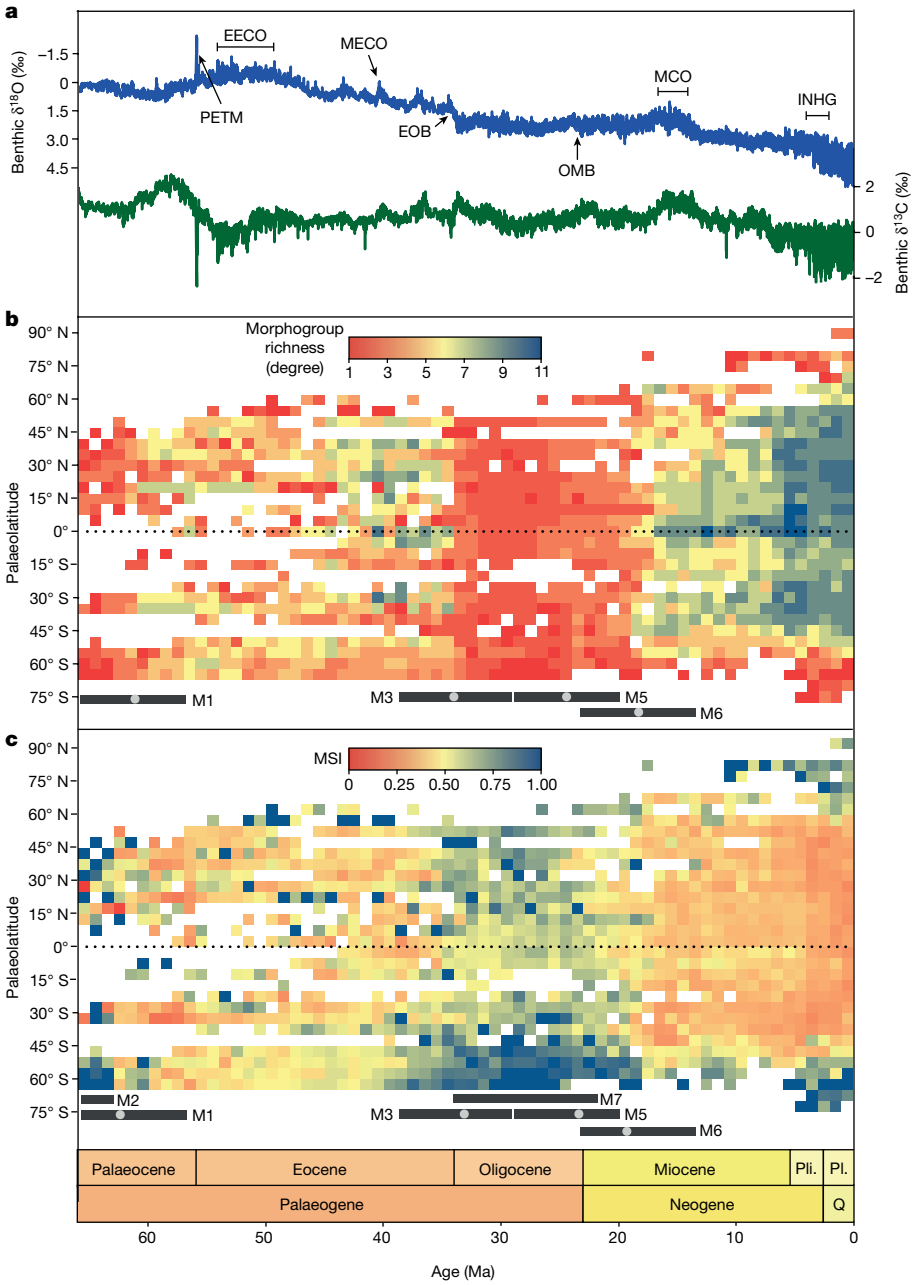

Fig. 3 | Cenozoic climate and morphogroup metrics. a, Benthic $\delta^{18}O$ and $\delta^{13}C$ from ref. 19. **b**, Morphogroup richness (degree or number of morphogroups), **c**, MSI. Note that in **b**,**c** the Northern Hemisphere bins extend to 90° N whereas the Southern Hemisphere bins extend to 75° S. Blue colours equal high morphogroup richness (**b**) or specialization (**c**), whereas red colours correspond to low values of each metric. The events of interest are noted in **b**,**c**—M1: post-K/Pg morphogroup recovery with increasing (morphogroup) richness in **b** and decreasing MSI in **c** (grey circles on the bars show the point of inflection in each case here and in M3–M6); M2: endemism or high specialization in southern mid–high latitudes (66–63 Ma); M3: rapid decrease in richness in **b** and increase in MSI in **c** at the Eocene–Oligocene boundary; M4: minor recovery in richness in **b** and decrease in MSI in **c** just before the Oligocene–Miocene boundary; M6: major recovery in richness in **b** and decrease in MSI in the early Miocene in **c**; M7: high MSI in southern mid–high latitudes during the Oligocene.

Cenozoic—may be evidence for the rapid onset of ocean temperatures thermally inhibitive to marine life[35,36]. However, whether temperatures consistently inhibited low-latitude marine biodiversity during the background Cenozoic greenhouse (for example, ref. 11) remains inconclusive owing to a general lack of low-latitude palaeontological samples[2,4,12].

We explored this hypothesis with our ecogroup specialization indices (ESI and ecogroup paired difference index; Fig. 2c and Extended Data Fig. 3c) across the early Eocene, where low and Northern Hemisphere latitudes indicate greater specialization. We find that ecogroup specialization is significantly greater across all latitudes during the interval from 56 to 50 Ma than during both the preceding (62–56 Ma, $P < 10^{-11}$, one-tailed t-test) and the succeeding (50–44 Ma, $P < 10^{-14}$, one-tailed t-test) 6-Myr intervals. We hypothesize that the emergence of highly specialized ecogroup communities occurring from 56 to 50 Ma was driven by the sustained peak Cenozoic warmth associated with the EECO (for example, ref. 37). Unfortunately, the possibility that low-latitude surface waters were thermally inhibitive to biodiversity remains inconclusive owing to the lack of samples at low latitudes from this time; however, our network analyses support the possibility that the peak warmth of the greenhouse world inhibited ecological communities across much of the globe. Any marine LBG interpretations during

this interval[11] should be approached with caution until this low-latitude sampling gap has been addressed.

By contrast, Southern Hemisphere mid–high latitudes record the lowest ecogroup specialization values from 56 to 50 Ma, and we find that palaeolatitudes 50–65° S differ significantly from all other regions ($P < 10^{-12}$, one-tailed *t*-test), where low and Northern Hemisphere latitudes are dominated by symbiont-bearing mixed layer dwellers (ecogroup 1) producing a LEG exhibiting a unimodal trough in the Southern Hemisphere (Extended Data Fig. 6a). We suggest that cooler, higher latitudes of the Southern Hemisphere may have acted as ecological refugia during the peak of Cenozoic warming, where greater thermal heterogeneity across this region potentially allowed for the development of vertical temperature gradients with greater niche partitioning and a more efficient biological pump able to support more equitable ecogroup communities[38]. These observations are also consistent with trait-based ecosystem models for this time period, which suggest increased export production and mean cell size among plankton communities, particularly across southern high palaeolatitudes[39]. Within lower and Northern Hemisphere palaeolatitudes, the high ecogroup specialization, due to a dominance of mixed layer-dwelling symbiont bearers (Fig. 1), suggests the presence of oligotrophic surface waters with poor vertical mixing and nutrient delivery to deeper depths consistent with higher sea surface temperatures[40].

Ecogroup richness is greatest in mid–high palaeolatitudinal regions during the peak of the EECO. As the middle Eocene progressed, ecogroup richness seems to show latitudinal contraction of a similar scale to the late Neogene patterns observed in ref. 1; this contraction preceded the increased MSI observed in the late Eocene discussed in the next section (Fig. 3c and Extended Data Fig. 3b). Unexpectedly, unlike the late Neogene cooling, which triggered an equatorward shift in ecogroup specialization indices and 'diversification in place' within ecogroup richness[1] (Fig. 2c), this mid-Eocene cooling triggered an equatorward shift for ecogroup richness (Fig. 2b), despite both intervals being typified by steepening latitudinal temperature gradients[41]. This observation yields two important implications. First, the long-term deep sea cooling trend, the 'descent into the icehouse', established from about 50 Ma[19,42] began detrimentally affecting ecological systems millions of years before the observed changes in global morphological metrics associated with the EOT (about 34 Ma, next section). Second, the global response of functional ecological groups to the same abiotic selection pressures (steepening latitudinal temperature gradients) may be entirely dependent on the background climatic state (for example, greenhouse or icehouse) to which a particular group is adapted. The latter would imply that the best analogue for the response of modern plankton to ongoing warming is ephemeral warming events after the Oligocene establishment of coolhouse and icehouse conditions such as the Miocene Climatic Optimum (Figs. 2a and 3a), rather than Palaeogene hyperthermals.

Re-establishment among EOT morphogroups

Morphogroup network metrics and richness observations leading up to the EOT (about 34 Ma) are disentangled from one another. Regions of high morphogroup specialization document a gradual increase, especially within the Southern Hemisphere, before the EOT (Fig. 3c and Extended Data Fig. 3b). Logistic regressions make clear that the most rapid increase in MSI (logistic inflection at 35.7 ± 0.7 Ma, $P < 0.05$; Fig. 3b,c and Extended Data Fig. 5) precedes the most rapid reduction in richness by about 2 Myr (inflection at 33.7 ± 0.1 Ma, $P < 0.05$); however, the reduction in richness is more rapid (absolute scaling constant has a slightly higher value for MSI; richness = 0.7016 ± 0.1040 and MSI = 1.0448 ± 0.3632). This shift among morphological communities directly followed the termination of the Middle Eocene Climatic Optimum (Fig. 2; about 40.5–40.1 Ma[19]), a transient period of global warming that was succeeded by significant cooling of sea surface temperatures approaching the EOT, especially within higher latitudes[41,43,44]. We suggest that this observed discrepancy between the hemispheres may signify post-Middle Eocene Climatic Optimum migration northward of regions suitable for equitable planktonic foraminiferal morphogroup communities (morphotones), similar to observations of late Cenozoic ecotones[2], although in this case isolated to the Southern Hemisphere (Fig. 3c). Owing to the tectonic opening of Southern Ocean gateways, and associated inception of the Antarctic Circumpolar Current[45,46], the Southern Hemisphere may have experienced more amplified latitudinal temperature gradients, sea surface environments and productivity flux at this time, triggering the shift in these communities[46–49]. Note, however, that comparable Northern Hemisphere palaeolatitudes are not as well represented throughout this interval in Triton (Fig. 3), and the presence of markedly heightened low-latitude species Shannon diversity for the entire Oligocene (Extended Data Fig. 4a) may indicate the retention of thermal niche stability among EOT survivor taxa that converged on the Equator to eke out the last remnant niches of the Cenozoic greenhouse. This observation warrants further investigation, where we are now observing contrasting biogeographic shifts in response to anthropogenic climate warming[6].

At the EOT (about 34 Ma[47]), morphogroup specialization metric values exhibit only a moderate increase (Fig. 3c and Extended Data Fig. 3b), whereas morphogroup richness is severely reduced across all latitudes (Fig. 3b). This latter pattern signifies the extinction of about 35% of macroperforate planktonic foraminiferal species[14,31] and more than 50% of total planktonic foraminiferal species over about 2 Myr[21,32], with losses being most severe among morphologically complex forms such as tubulospinate *Hantkenina* and *Cribrohantkenina*, and keel-bearing *Turborotalia* occupying the upper water column[14,32,50]. The following period of morphological 'stasis' was typified by foraminifera genera with simple globular morphologies such as *Dentoglobigerina, Paragloborotalia* and *Subbotina*, and lasted until the end of the Oligocene[14,22,31,32] (Fig. 3b).

Following the EOT, Southern Hemisphere high and mid latitudes maintained heightened MSI (and morphogroup paired difference index), as well as Simpson's evenness[2], for much of the Oligocene and early Miocene, where once more, like during the EECO, we document an LEG with a unimodal trough located in the Southern Hemisphere (Extended Data Fig. 6b). However, we note minor changes in both morphogroup richness (inflection at 25.0 ± 0.2 Ma, $P < 10^{-6}$) and MSI (inflection at 23.4 ± 0.5 Ma, $P < 10^{-5}$) during the late Oligocene (Fig. 3). Furthermore, through the Oligocene (34–23 Ma), palaeolatitudes from 50 to 65° S differed from all other regions for MSI ($P < 10^{-12}$, one-tailed *t*-test), but not for morphogroup richness ($P = 0.13$).

At the EOT, latitudinal temperature gradients steepened through high-latitude sea surface temperature cooling[51]. However, model–data comparisons indicate consistently low latitudinal temperature gradients for the duration of the Oligocene[41,47]. Despite this global thermal stability, richness and specialization among morphogroups changed little well into the Oligocene (Fig. 3), where the rebound of metrics for macroperforate planktonic foraminifera occurred millions of years later than the increase observed following the K/Pg event, which triggered a much greater and more rapid decline in diversity than the EOT[22,32]. We suggest this discrepancy to be the result of the differing nature of these events. The K/Pg extinction event was a severe but ephemeral change. Once ecological recovery commenced and ecosystem function was restored, the underlying physicochemical state of this greenhouse ocean mirrored its pre-event character, allowing biodiversity to recreate niches that had been destroyed by the extinction. The EOT on the other hand represents a global state change from greenhouse to icehouse. Planktonic foraminifera evolved in the Jurassic (for example, ref. 32) and their entire evolutionary history up to this point was spent in hothouse or greenhouse oceans, with fundamentally different latitudinal and vertical ocean structure than during the Oligocene[19,22]. The extended delay in morphogroup diversity following

the EOT may represent the prerequisite accumulation of new genetic diversity and phenotypes among the survivors in the newly established icehouse ocean state, ultimately allowing for late Oligocene diversification (Fig. 3).

Riddle of early Miocene morphogroups

At about 18.5 Ma, morphogroup specialization decreases rapidly (inflection at 19.0 ± 0.5 Ma, $P < 0.05$) and morphogroup richness increases rapidly (inflection at 18.4 ± 0.1 Ma, $P < 0.01$). The latter of these two changes was no doubt triggered by the evolution of *Globoconella* and *Hirsutella*. The homoplastic morphological reacquisition of a peripheral keel in these taxa, thought to be an adaptation for the exploitation of deeper habitats, ultimately ushered in the mid-Miocene exploitation of deep-water niches[1,2,52,53]. These morphogroup changes also approximate the interval within which recent work revealed global declines in shark populations (abundance loss >90%[5]) and sharp decreases in the $\delta^{15}N$ of foraminifera-bound organic matter[54], and the Tethys Seaway finally closed[55]. Our data, along with observations in refs. 5,54, suggest that substantial changes in the palaeoceanography, community dynamics and oceanic nutrient structure of global pelagic ecosystems all occurred around 19 Ma. Further work is underway to determine the environmental mechanisms at play.

Renewal of mid-Miocene ecogroups and morphogroups

Important changes in global palaeoceanography over the past 15 Myr proved fundamental to the origination and polar amplification of the modern marine LBG among calcareous plankton through evolutionary exploitation, speciation and community migration[1,2,52,53,56,57].

There was a delay between the initial mid-Miocene colonization of new ecological niches, and diversification within those niches, in line with the results from previous works[21] for the aftermath of the K/Pg mass extinction event and the EOT. Following a diversification pulse at about 15 Ma, it is not until about 10 Ma that the proportion of planktonic foraminiferal communities occupying deeper waters greatly increased and the evolution of deeper-dwelling planktonic foraminifera accelerated, with heightened origination rates for about 5 Myr leading to a late Cenozoic diversity peak at about 5 Ma[1,2,22,31,53,56,58]. However, unlike the aftermath of the K/Pg event, where the evolutionary innovations such as muricate, spinose walls permitted the exploitation of the newly oligotrophic shallow mixed layer, this mid-Miocene niche propagation involved the exploitation of deeper waters now exhibiting reduced oligotrophy, and required morphological adaptations such as the development of marginal keels in the *Fohsella, Hirsutella* and *Menardella* clades, and digitate chambers in *Beella*[52,53].

Notably, many of the new deeper-dwelling species that originated during this bathymetric radiation exhibited biogeographic ranges restricted almost entirely to mid latitudes. Whereas some species that evolved in the Southern Hemisphere remained there exclusively[55], others eventually migrated to the Northern Hemisphere[58]. Deepening food and oxygen availability[52,53], coupled with the unique nature of Southern Hemisphere palaeoceanography, may have erected localized gene flow barriers robust enough to facilitate allopatric pelagic speciation followed by eventual hemispheric dispersion[58,59]. Conditions more conducive to restricting gene flow may explain the lower ESI values, and higher ecogroup and morphogroup richness earlier in the Miocene, all of which are not observed in the Northern Hemisphere until a little later (Figs. 2b and 3b).

Conclusion

Our work provides new interpretations of the structural and temporal evolution of LEGs and functional pelagic communities over geological time, discerning the impacts of climatic perturbation effects on ecological and morphological traits in the planktonic foraminifera. This detailed, global perspective spanning the whole Cenozoic is a substantial step change from studies of individual time intervals based on individual or groups of sites, and is made possible only because of the extensive temporal and latitudinal resolution of the Triton dataset[4], and the use of a bipartite network framework that allowed us to take a systems perspective to quantify various aspects of functional group diversity, latitudinal specialization and latitudinal equitability. Our results demonstrate important biogeographic patterns in deep time such as low-latitude specialization under both greenhouse and icehouse states, as well as globally spanning equatorward migrations indicating extensive heterogeneity across ecological and morphological functional groups. Here, our network analyses record that global changes in functional group specialization indices associated with the aftermath of the K/Pg extinction event, the EECO, the EOT, the early Miocene and the middle Miocene, often precede, or are entirely uncorrelated with, those in functional richness metrics. However, despite the global extent of these patterns, we demonstrate evidence for endemism after the K/Pg mass extinction, refugia during the peak of the Cenozoic hothouse, and specialization during the descent into the icehouse restricted entirely to southern palaeolatitudes, indicating significant hemispheric heterogeneity within climate and biodiversity for much of the Cenozoic (for example, refs. 30,33,38,39,41,43,44,46,48,49). Moreover, the global biogeographic response of the group is unique to the same abiotic force (steepening latitudinal temperature gradients), suggesting that ecosystem responses may depend on the phylogenetic group.

All of the studied Cenozoic perturbations are noted for important changes within the structure of the ocean and/or marine biological carbon pump, and all exhibit distinct signals within our network and richness metrics. However, the magnitude, timing and sequence of change are unique for each event. This is significant as current anthropogenic climate trends retain the capacity to melt modern continental-scale ice sheets that hold the meltwater potential to markedly disrupt global ocean circulation patterns, nutrient distributions and water column structure (for example, ref. 60). As the effects of imminent future changes in our climate and marine environment begin to take shape, changes in community-scale patterns within functional groups may represent precursory signals of ecosystem change, before major richness losses.

Ancient patterns in the highly resolved spatiotemporal record of microfossil groups may provide a fossil analogue to the systemic global changes being driven by anthropogenic climate forcing at present[17]. A key finding of our work is that the response to climate events may depend on the background state, as the response to steepening latitudinal temperature gradients followed opposite patterns in the greenhouse Eocene and icehouse Neogene. As modern latitudinal temperature gradients lessen, warming periods in an icehouse climate state may provide the best analogue to inform policy decisions and pathway projections. Accordingly, research priorities should be to quantify the pre-industrial LEGs and global community structure for different taxa across pelagic food webs and determine how these structures have been altered by human-induced climate forcing. Also needed is research to assess ancient community tipping points that precede extinction, as continued monitoring of modern spatial distributions within functional groups may present an early warning system capable of identifying regions in need of greater and faster mitigation of anthropogenic climate effects on biodiversity.

Online content

Any methods, additional references, Nature Portfolio reporting summaries, source data, extended data, supplementary information, acknowledgements, peer review information; details of author contributions

and competing interests; and statements of data and code availability are available at https://doi.org/10.1038/s41586-024-07337-9.

1. Woodhouse, A., Swain, A., Fagan, W. F., Fraass, A. J. & Lowery, C. M. Late Cenozoic cooling restructured global marine plankton communities. *Nature* **614**, 713–718 (2023).
2. Fenton, I. S., Aze, T., Farnsworth, A., Valdes, P. & Saupe, E. E. Origination of the modern-style diversity gradient 15 million years ago. *Nature* **614**, 708–712 (2023).
3. Jablonski, D., Roy, K. & Valentine, J. W. Out of the tropics: evolutionary dynamics of the latitudinal diversity gradient. *Science* **314**, 102–106 (2006).
4. Fenton, I. S. et al. Triton, a new species-level database of Cenozoic planktonic foraminiferal occurrences. *Sci. Data* **8**, 160 (2021).
5. Sibert, E. C. & Rubin, L. D. An early Miocene extinction in pelagic sharks. *Science* **372**, 1105–1107 (2021).
6. Jonkers, L., Hillebrand, H. & Kucera, M. Global change drives modern plankton communities away from the pre-industrial state. *Nature* **570**, 372–375 (2019).
7. Benedetti, F. et al. Major restructuring of marine plankton assemblages under global warming. *Nat. Commun.* **12**, 5226 (2021).
8. Yasuhara, M. et al. Past and future decline of tropical pelagic biodiversity. *Proc. Natl Acad. Sci. USA* **117**, 12891–12896 (2020).
9. Fenton, I. S., Pearson, P. N., Dunkley Jones, T. & Purvis, A. Environmental predictors of diversity in recent planktonic foraminifera as recorded in marine sediments. *PLoS ONE* **11**, e0165522 (2016).
10. Fenton, I. S. et al. The impact of Cenozoic cooling on assemblage diversity in planktonic foraminifera. *Philos. Trans. R. Soc. B* **371**, 20150224 (2016).
11. Raja, N. B. & Kiessling, W. Out of the extratropics: the evolution of the latitudinal diversity gradient of Cenozoic marine plankton. *Proc. R. Soc. B* **288**, 20210545 (2021).
12. Brodie, J. F. & Mannion, P. D. The hierarchy of factors predicting the latitudinal diversity gradient. *Trends Ecol. Evol.* **38**, 15–23 (2023).
13. Chaudhary, C., Saeedi, H. & Costello, M. J. Bimodality of latitudinal gradients in marine species richness. *Trends Ecol. Evol.* **31**, 670–676 (2016).
14. Aze, T. et al. A phylogeny of Cenozoic macroperforate planktonic foraminifera from fossil data. *Biol. Rev.* **86**, 900–927 (2011).
15. Tittensor, D. P. et al. Global patterns and predictors of marine biodiversity across taxa. *Nature* **466**, 1098–1101 (2010).
16. Edie, S. M., Jablonski, D. & Valentine, J. W. Contrasting responses of functional diversity to major losses in taxonomic diversity. *Proc. Natl Acad. Sci. USA* **115**, 732–737 (2018).
17. Pörtner, H.-O. et al. in *Climate Change 2022: Impacts, Adaptation, and Vulnerability* (IPCC, Cambridge Univ. Press, 2022).
18. Jones, H. L., Lowery, C. M. & Bralower, T. J. Delayed calcareous nannoplankton boom-bust successions in the earliest Paleocene Chicxulub (Mexico) impact crater. *Geology* **47**, 753–756 (2019).
19. Westerhold, T. et al. An astronomically dated record of Earth's climate and its predictability over the last 66 million years. *Science* **369**, 1383–1387 (2020).
20. Kirchner, J. W. & Weil, A. Delayed biological recovery from extinctions throughout the fossil record. *Nature* **404**, 177–180 (2000).
21. Lowery, C. M. & Fraass, A. J. Morphospace expansion paces taxonomic diversification after end Cretaceous mass extinction. *Nat. Ecol. Evol.* **3**, 900–904 (2019).
22. Lowery, C. M., Bown, P. R., Fraass, A. J. & Hull, P. M. Ecological response of plankton to environmental change: thresholds for extinction. *Annu. Rev. Earth Planet. Sci.* **48**, 403–429 (2020).
23. Birch, H. S., Coxall, H. K., Pearson, P. N., Kroon, D. & Schmidt, D. N. Partial collapse of the marine carbon pump after the Cretaceous-Paleogene boundary. *Geology* **44**, 287–290 (2016).
24. Birch, H., Schmidt, D. N., Coxall, H. K., Kroon, D. & Ridgwell, A. Ecosystem function after the K/Pg extinction: decoupling of marine carbon pump and diversity. *Proc. R. Soc. B* **288**, 20210863 (2021).
25. Alvarez, S. A. et al. Diversity decoupled from ecosystem function and resilience during mass extinction recovery. *Nature* **574**, 242–245 (2019).
26. Gibbs, S. J. et al. Algal plankton turn to hunting to survive and recover from end-Cretaceous impact darkness. *Sci. Adv.* **6**, eabc9123 (2020).
27. Birch, H. S., Coxall, H. K. & Pearson, P. N. Evolutionary ecology of Early Paleocene planktonic foraminifera: size, depth, habitat and symbiosis. *Paleobiology* **38**, 374–390 (2012).
28. Pearson, P. N., John, E., Wade, B. S., D'haenens, S. & Lear, C. H. Spine-like structures in Paleogene muricate planktonic foraminifera. *J. Micropalaeontol.* **41**, 107–127 (2022).
29. Coxall, H. K., D'Hondt, S. & Zachos, J. C. Pelagic evolution and environmental recovery after the Cretaceous-Paleogene mass extinction. *Geology* **34**, 297–300 (2006).
30. Quillévéré, F., Norris, R. D., Moussa, I. & Berggren, W. A. Role of photosymbiosis and biogeography in the diversification of early Paleogene acarninids (planktonic foraminifera). *Paleobiology* **27**, 311–326 (2001).
31. Ezard, T. H. G., Aze, T., Pearson, P. N. & Purvis, A. Interplay between changing climate and species' ecology drives macroevolutionary dynamics. *Science* **332**, 349–351 (2011).
32. Fraass, A. J., Kelly, D. C. & Peters, S. E. Macroevolutionary history of the planktic foraminifera. *Annu. Rev. Earth Planet. Sci.* **43**, 139–166 (2015).
33. Huber, B. T., Petrizzo, M. R. & MacLeod, K. G. Planktonic foraminiferal endemism at southern high latitudes following the terminal Cretaceous extinction. *J. Foraminiferal Res.* **50**, 382–402 (2020).
34. Huber, B. T., MacLeod, K. G., Watkins, D. K. & Coffin, M. F. The rise and fall of the Cretaceous Hot Greenhouse climate. *Global Planet. Change* **167**, 1–23 (2018).
35. Speijer, R., Scheibner, C., Stassen, P. & Morsi, A. M. M. Response of marine ecosystems to deep-time global warming: a synthesis of biotic patterns across the Paleocene-Eocene thermal maximum (PETM). *Austrian J. Earth Sci.* **105**, 6–16 (2012).
36. Aze, T. Unraveling ecological signals from a global warming event of the past. *Proc. Natl Acad. Sci. USA* **119**, e2201495119 (2022).
37. Silva, I. P. & Boersma, A. Atlantic Paleogene planktonic foraminiferal bioprovincial indices. *Mar. Micropaleontol.* **14**, 357–372 (1989).
38. Douglas, P. M. et al. Pronounced zonal heterogeneity in Eocene southern high-latitude sea surface temperatures. *Proc. Natl Acad. Sci. USA* **111**, 6582–6587 (2014).
39. Wilson, J. D., Monteiro, F. M., Schmidt, D. N., Ward, B. A. & Ridgwell, A. Linking marine plankton ecosystems and climate: a new modeling approach to the warm early Eocene climate. *Paleoceanogr. Paleoclimatol.* **33**, 1439–1452 (2018).
40. John, E. H. et al. Warm ocean processes and carbon cycling in the Eocene. *Philos. Trans. R. Soc. A* **371**, 20130099 (2013).
41. Gaskell, D. E. et al. The latitudinal temperature gradient and its climate dependence as inferred from foraminiferal $\delta^{18}O$ over the past 95 million years. *Proc. Natl Acad. Sci. USA* **119**, e2111332119 (2022).
42. Thomas, E. Descent into the Icehouse. *Geology* **36**, 191–192 (2008).
43. Schmidt, D. N., Lazarus, D., Young, J. R. & Kucera, M. Biogeography and evolution of body size in marine plankton. *Earth Sci. Rev.* **78**, 239–266 (2006).
44. Inglis, G. N. et al. Descent toward the Icehouse: Eocene sea surface cooling inferred from GDGT distributions. *Paleoceanography* **30**, 1000–1020 (2015).
45. Scher, H. D. & Martin, E. E. Timing and climatic consequences of the opening of Drake Passage. *Science* **312**, 428–430 (2006).
46. Houben, A. J., Bijl, P. K., Sluijs, A., Schouten, S. & Brinkhuis, H. Late Eocene Southern Ocean cooling and invigoration of circulation preconditioned Antarctica for full-scale glaciation. *Geochem. Geophys. Geosyst.* **20**, 2214–2234 (2019).
47. Hutchinson, D. K. et al. The Eocene–Oligocene transition: a review of marine and terrestrial proxy data, models and model–data comparisons. *Clim. Past* **17**, 269–315 (2021).
48. Rabosky, D. L. & Sorhannus, U. Diversity dynamics of marine planktonic diatoms across the Cenozoic. *Nature* **457**, 183–186 (2009).
49. Ladant, J. B., Donnadieu, Y., Bopp, L., Lear, C. H. & Wilson, P. A. Meridional contrasts in productivity changes driven by the opening of Drake Passage. *Paleoceanogr. Paleoclimatol.* **33**, 302–317 (2018).
50. Coxall, H. K. & Pearson, P. N. in *Deep-Time Perspectives on Climate Change: Marrying the Signal from Computer Models and Biological Proxies* (eds Williams, M. et al.) 351–387 (The Micropalaeontological Society, 2007).
51. Śliwińska, K. K. et al. Sea surface temperature evolution of the North Atlantic Ocean across the Eocene–Oligocene transition. *Clim. Past* **19**, 123–140 (2023).
52. Boscolo-Galazzo, F. et al. Temperature controls carbon cycling and biological evolution in the ocean twilight zone. *Science* **371**, 1148–1152 (2021).
53. Boscolo-Galazzo, F. et al. Late Neogene evolution of modern deep-dwelling plankton. *Biogeosciences* **19**, 743–762 (2022).
54. Auderset, A. et al. Enhanced ocean oxygenation during Cenozoic warm periods. *Nature* **609**, 77–82 (2022).
55. Yasuhara, M. et al. Hotspots of Cenozoic tropical marine biodiversity. *Oceanogr. Mar. Biol.* **60**, 243–300 (2022).
56. Kucera, M. & Schönfeld, J. in *Deep-Time Perspectives on Climate Change: Marrying the Signal from Computer Models and Biological Proxies* (eds Williams, M. et al.) 409–425 (The Micropalaeontological Society, 2007).
57. Yasuhara, M. & Deutsch, C. A. Tropical biodiversity linked to polar climate. *Nature* **614**, 626–628 (2023).
58. Lam, A. R., Crundwell, M. P., Leckie, R. M., Albanese, J. & Uzel, J. P. Diachroneity rules the mid-latitudes: a test case using late Neogene planktic Foraminifera across the Western Pacific. *Geosciences* **12**, 190 (2022).
59. Scott, G. H., Bishop, S. & Burt, B. J. *Guide to some Neogene Globorotalids (Foraminiferida) from New Zealand* (New Zealand Geological Survey, 1990).
60. Golledge, N. R. et al. Global environmental consequences of twenty-first-century ice-sheet melt. *Nature* **566**, 65–72 (2019).

Methods

Triton database and related metadata

We used the Triton dataset[5,61–64] in this study, excluding all 38,046 occurrences (7.4% of the total data) of taxa exhibiting microperforate and medioperforate wall textures owing to a less refined phylogeny compared to macroperforate forms[14,65]. All macroperforate planktonic foraminiferal species were assigned speciation and extinction datums in accordance with refs. 4,14 and all species occurrences located outside the assigned stratigraphic ranges were removed to eliminate much of the occurrence data probably attributable to misidentification and/or reworking that may create artificial 'tails' within speciation and extinction data[66,67], leaving a dataset containing 359,253 entries. All planktonic foraminiferal age data were assigned to 1-Myr time bins to assess patterns in network dynamics. Furthermore, all planktonic foraminiferal spatial data were binned to palaeolatitudinal bands spanning 5 decimal degrees. Species were also allocated to the specified 'ecogroups' and 'morphogroups' (Fig. 1) of ref. 14 to determine whether species ecology and morphology had a role in their biogeographic network interactions throughout the Cenozoic.

Ecogroups are assigned on the basis of species biogeographic distributions, as well as stable isotopic oxygen ($\delta^{18}O$) and carbon ($\delta^{13}C$) signatures of planktonic foraminifera shells. These isotopic ratios can help determine the relative degree of bathymetric and ecological separation within extant and extinct species. In turn, we can infer species-specific ecological niches due to different physicochemical and biological processes and variations with depth in the water column[3,14,68–71]. Ecogroups are defined as follows—ecogroup 1: open ocean surface mixed layer dwellers with algal photosymbionts; ecogroup 2: open ocean surface mixed layer dwellers without algal photosymbionts; ecogroup 3: open ocean thermocline dwellers; ecogroup 4: open ocean sub-thermocline dwellers; ecogroup 5: high-latitude dwellers; ecogroup 6: high-productivity- or upwelling-region dwellers[14] (Fig. 1).

Morphogroups comprise 19 separate forms based on external, often functional characters of shells[14,27] (species silhouettes are modified from Huber et al.[72] and Young et al.[73]). Combined, ecogroups and morphogroups allow us to infer the habitability, niche partitioning and vertical structure of the water column through different periods of geological time and their relationship with global palaeoceanography and biodiversity[2,3,71,74]. The palaeoceanographic and macroevolutionary significance of the sequential and sometimes iterative evolution of Cenozoic planktonic foraminiferal functional groups has long been recognized (for example, refs. 75,76); however, modern advances in statistical palaeobiology and the creation of Triton[4] now permit the analyses of the globally spanning responses of this plankton group at a higher spatiotemporal resolution than ever before.

Calculating network-associated ecological metrics

The modified Triton dataset was formatted to bin macroperforate planktonic foraminiferal occurrences at every 1-Myr interval in time and 5° of palaeolatitude in space as described above. All data at every time interval (1-Myr bin) were used to construct bipartite networks with palaeolatitude as one node class and either ecogroup or morphogroup as the other node class[3,77]. The links between these nodes denoted the presence of a particular ecogroup or morphogroup in a given palaeolatitudinal band, and the width of these links denoted the number of occurrences of that ecogroup or morphogroup in the specific palaeolatitudinal band. To test for the sampling completeness of the dataset at the resolution of interest, we looked at the sampling coverage of the associations (frequency of each unique morphogroup or ecogroup in a palaeolatitudinal band) in each time bin (1 Myr) using the iNEXT package[78] for both morphogroups and ecogroups.

We then used the bipartite package[79] in R v4.2.2 to calculate three metrics for each palaeolatitudinal band node: the degree for each palaeolatitudinal band node (that is, number of ecogroups or morphogroups at that palaeolatitudinal band); the ESI and MSI; and the ecogroup and morphogroup paired difference index (EPDI and MPDI). ESI/MSI is the coefficient of variation of number of occurrences of ecogroups or morphogroups in a given palaeolatitudinal band, normalized to values between 0 and 1, in which 0 denotes low and 1 denotes a high variability (and therefore, low and high specificity, or functional communities being generalized and specialized, respectively). ESI/MSI is directly based on the idea of the species specificity index from refs. 80,81, and in our context, measures how equitable or even the distribution of ecogroups or morphogroups is in a given palaeolatitudinal band (for a given time bin). A band having exactly the same number of occurrences of all groups will have a zero value of ESI or MSI and a band having only one dominant group will have values closer to 1. EPDI/MPDI also measures the equitability of groups, and is mathematically the same as the paired difference index described in ref. 81. The last metric accounts for the fact that abundances may have varying statistical distributions, and therefore, no single variability measure can be applied equally to all data. EPDI or MPDI contrasts a group's highest abundance in a given palaeolatitudinal band to that of other groups in the palaeolatitudinal band for a given time bin[81].

In addition Shannon diversity metrics were calculated for species, morphogroups and ecogroups using the vegan package in R[82].

Statistical analysis

To quantify the statistical extent of certain patterns that were visually discernible and were supported by our prior reading of literature, we carried out further analyses using the base statistical features of R v4.2.2.

To look at the recovery in post-K/Pg morphogroups, we fitted a logistic function to the normalized averaged morphogroup richness and MSI from 66–56-Ma bins (averaged across all latitudes for a given time bin). We used a standard maximum–minimum normalization (for data within this interval) and carried out the fitting using nls and SSlogis functions. We postulated the high southern palaeolatitudes (50–65° S) to have a different pattern than the rest, especially in the first 3 Myr post-K/Pg boundary. To test this, we used a one-tailed *t*-test with unequal variances to examine differences between the pooled values of MSI for these higher southern latitudes and those of other latitudes during 66–64-Ma bins.

We theorized that ESI (and EPDI) would increase globally following the initiation of the PETM (about 56 Ma), which continued until the termination of the EECO (about 53.3–49.1 Ma). To test this, we used *t*-tests (one-tailed with unequal variances) to compare the pooled values of ESI (and EPDI) across all latitudes in the period before the initiation of PETM (62–56 Ma) to those during the PETM–EECO interval (56–50 Ma), and separately to compare those of the PETM–EECO interval to those in the post-EECO interval (50–44 Ma). We also proposed the existence of Southern Hemisphere refugia during the PETM–EECO interval, and used a *t*-test (one-tailed with unequal variances) to examine differences in pooled ESI (or EPDI) values between those of high southern palaeolatitudes (50–65° S) and other latitudes.

To characterize the decrease in morphogroup richness and MSI across the EOT, we fitted a logistic function to the normalized averaged morphogroup richness and MSI from 39–29-Ma bins (averaged across all latitudes for a given time bin) using the same logistic functions as in the post-K/Pg analysis. We also repeated the same analysis during the Oligocene–Miocene boundary using the bins from 24–14 Ma.

Furthermore, to test the distinctive patterns of morphogroup richness and MSI in the southern oceans across the EOT, we used *t*-tests (one-tailed, unequal variances) to differentiate the planktonic community structure of the high southern palaeolatitudes (50–65° S) from those of other latitudes.

To evaluate whether the differences in total number of fossil occurrences across the sampled time frame were driving the patterns

observed in our study, we resampled the data from the past 66 Myr (see ref. 83 for resampling details). For each of the three cases, we resampled without replacement, and in such a way that the total number of occurrences in each 1-Myr time bin equalled the smallest number of occurrences in any 1-Myr time bin in that case. Then, we constructed networks and calculated network metrics for each resampling case. We repeated this entire procedure 500 times for each 1-Myr time slice, and then averaged the values obtained by palaeolatitudinal band per time bin and compared them to the metrics obtained from the empirical dataset. Across all network metrics, relative changes averaged less than 10% for all of the metrics between the resampled datasets and the original dataset until 58 Ma. Beyond 58 Ma, resampling for each time bin to the lowest occurrence value in any time bin yielded changes <20%. These larger changes mean that, beyond 58 Ma, interpretations must be cautious because of lower sampling intensity. Note, however, that the major patterns presented here hold true despite changes in the metrics during times >58 Ma. We therefore conclude that sampling differences across time were not, in general, driving the patterns observed.

Reporting summary

Further information on research design is available in the Nature Portfolio Reporting Summary linked to this article.

Data availability

All data were sourced from the Triton dataset[4] (https://doi.org/10.1038/s41597-021-00942-7).

Code availability

The code used to carry out the analyses is available in Zenodo at https://doi.org/10.5281/zenodo.7888565 (ref. 84).

61. Lazarus, D. Neptune: a marine micropaleontology database. *Math. Geol.* **26**, 817–832 (1994).
62. Spencer-Cervato, C. The Cenozoic deep sea microfossil record: explorations of the DSDP/ODP sample set using the Neptune database. *Palaeontol. Electron.* **2**, a13 (1999).
63. Siccha, M. & Kucera, M. ForCenS, a curated database of planktonic foraminifera census counts in marine surface sediment samples. *Sci. Data* **4**, 170109 (2017).
64. Renaudie, J., Lazarus, D. B. & Diver, P. NSB (Neptune Sandbox Berlin): an expanded and improved database of marine planktonic microfossil data and deep-sea stratigraphy. *Palaeontol. Electron.* **23**, a11 (2020).
65. Pearson, P. N. in *Atlas of Oligocene Planktonic Foraminifera* Special Publication No. 46 (eds Wade, B. S. et al.) 415–428 (Cushman Foundation of Foraminiferal Research, 2018).
66. Liow, L. H., Skaug, H. J., Ergon, T. & Schweder, T. Global occurrence trajectories of microfossils: environmental volatility and the rise and fall of individual species. *Paleobiology* **36**, 224–252 (2010).
67. Lazarus, D., Weinkauf, M. & Diver, P. Pacman profiling: a simple procedure to identify stratigraphic outliers in high-density deep-sea microfossil dataPACMAN PROFILING. *Paleobiology* **38**, 144–161 (2012).
68. Birch, H., Coxall, H. K., Pearson, P. N., Kroon, D. & O'Regan, M. Planktonic foraminifera stable isotopes and water column structure: disentangling ecological signals. *Mar. Micropaleontol.* **101**, 127–145 (2013).
69. Woodhouse, A. *Evolutionary Dynamics of Cenozoic Planktonic Foraminifera: Insights from Biogeography, Geochemistry, and Morphology*. PhD thesis, Univ. Leeds (2021).
70. Woodhouse, A. et al. Adaptive ecological niche migration does not negate extinction susceptibility. *Sci. Rep.* **11**, 15411 (2021).
71. Woodhouse, A. et al. Paleoecology and evolutionary response of planktonic foraminifera to the mid-Pliocene Warm Period and Plio-Pleistocene bipolar ice sheet expansion. *Biogeosciences* **20**, 121–139 (2023).
72. Huber, B. T. et al. Pforams@ microtax. *Micropaleontology* **62**, 429–438 (2016).
73. Young, J. R. et al. Mikrotax: developing a genuinely effective platform for palaeontological geoinformatics. *Acta Geolog. Sin.* **93**, 70–72 (2019).
74. Yasuhara, M. & Deutsch, C. A. Tropical biodiversity linked to polar climate. *Nature* **614**, 626–628 (2023).
75. Cifelli, R. Radiation of Cenozoic planktonic foraminifera. *Syst. Zool.* **18**, 154–168 (1969).
76. Cita, M. B. & Premoli Silva, I. P. Planktonic foraminifers as ecologic indicators. Examples from the fossil record of the Mediterranean Sea and of the Atlantic Ocean. *Ital. J. Zool.* **45**, 115–131 (1978).
77. Swain, A., Maccracken, S. A., Fagan, W. F. & Labandeira, C. C. Understanding the ecology of host plant–insect herbivore interactions in the fossil record through bipartite networks. *Paleobiology* **48**, 239–260 (2021).
78. Hsieh, T. C., Ma, K. H. & Chao, A. iNEXT: an R package for rarefaction and extrapolation of species diversity (Hill numbers). *Methods Ecol. Evol.* **7**, 1451–1456 (2016).
79. Dormann, C. F., Fründ, J., Blüthgen, N. & Gruber, B. Indices, graphs and null models: analyzing bipartite ecological networks. *Open Ecol. J.* **2**, 7–24 (2009).
80. Julliard, R., Clavel, J., Devictor, V., Jiguet, F. & Couvet, D. Spatial segregation of specialists and generalists in bird communities. *Ecol. Lett.* **9**, 1237–1244 (2006).
81. Poisot, T., Canard, E., Mouquet, N. & Hochberg, M. E. A comparative study of ecological specialization estimators. *Methods Ecol. Evol.* **3**, 537–544 (2012).
82. Dixon, P. VEGAN, a package of R functions for community ecology. *J. Veg. Sci.* **14**, 927–930 (2003).
83. Swain, A. et al. Sampling bias and the robustness of ecological metrics for plant–damage-type association networks. *Ecology* **104**, e3922 (2023).
84. Swain, A. Biogeographic patterns in Cenozoic foram functional groups. *Zenodo* https://doi.org/10.5281/zenodo.7888565 (2023).

Acknowledgements A.S. and W.F.F. were supported by the University of Maryland, A.W. was supported by a postdoctoral fellowship at the University of Texas Institute for Geophysics, and A.J.F. receives funding from NSERC through DGECR-2022-00141 and RGPIN-2022-03305. A.S. additionally acknowledges training and technical support from the COMBINE programme at the University of Maryland, the James S. McDonnell Foundation and the Society of Fellows at Harvard University. We thank the creators of the Triton dataset—I. Fenton, T. Aze, D. Lazarus, J. Renaudie, A. Dunhill, J. Young and E. Saupe—without whom this study would not have been possible, as well as the micropalaeontologists and scientific ocean drilling staff who generated and contributed to the underlying data; and P. Pearson, J. Partin, S. D'Hondt, M. Leckie, E. Sibert and A. Auderset for scientific discussion of the manuscript.

Author contributions A.S. and A.W. formulated the study, generated the data and carried out the analyses. All authors contributed to the interpretation of data. A.S. and A.W. conceived and plotted the figures. A.S. wrote the code to carry out analyses. All authors contributed to the writing and editing of the manuscript.

Competing interests The authors declare no competing interests.

Additional information

Supplementary information The online version contains supplementary material available at https://doi.org/10.1038/s41586-024-07337-9.

Correspondence and requests for materials should be addressed to Anshuman Swain.

Peer review information *Nature* thanks Helen Coxall, Brian Huber, Moriaki Yasuhara and the other, anonymous, reviewer(s) for their contribution to the peer review of this work. Peer reviewer reports are available.

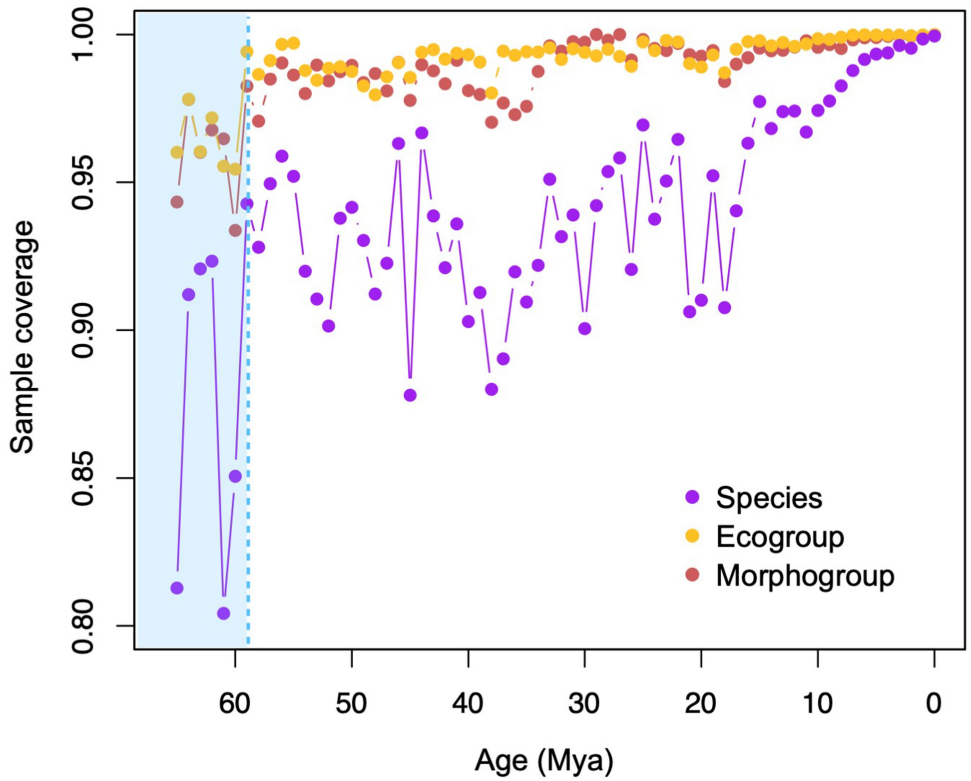

Extended Data Fig. 1 | Sampling completeness over time. Sample coverage values calculated for occurrences in different palaeolatitudinal bands for each million year slice for species, ecogroups and morphogroups. Note that small sample sizes limit confidence in estimates left of the blue dotted line (≥ 58 Ma). Also see Extended Data Fig. 2.

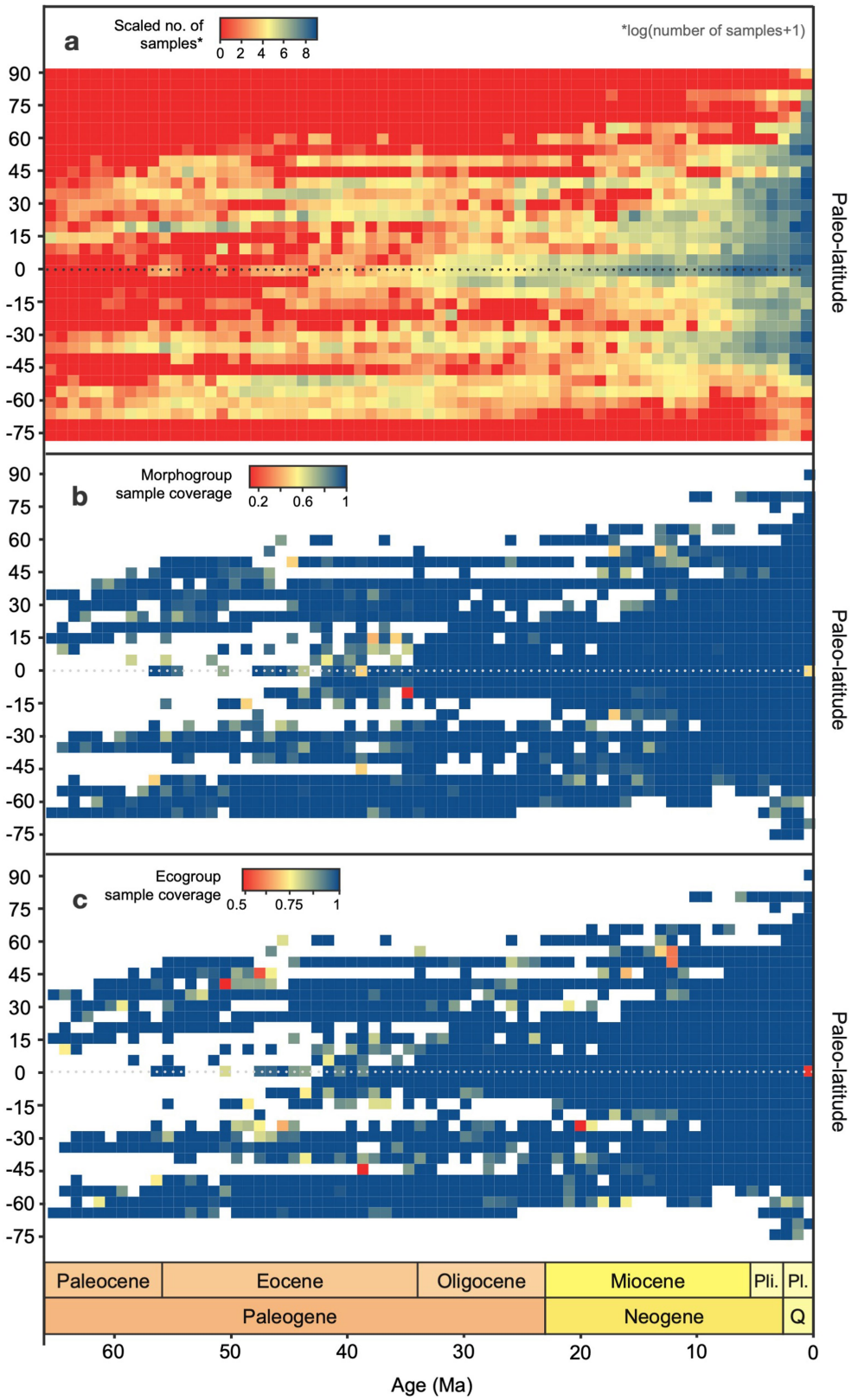

Extended Data Fig. 2 | Spatially-explicit sampling completeness over time. (A) Logarithmic scaling of total number of samples, (B) Sample coverage of morphogroups, (C) Sample coverage of ecogroups. Note that, as mentioned in Extended Data Fig. 1, the number of samples for (≥ 58 Ma) is quite low and therefore must be treated with caution. In (B) and (C), the palaeolatitudinal bands in a given time bin with less than 5 samples have been removed. Note that blue colors equal high values, whereas red colors correspond to low values.

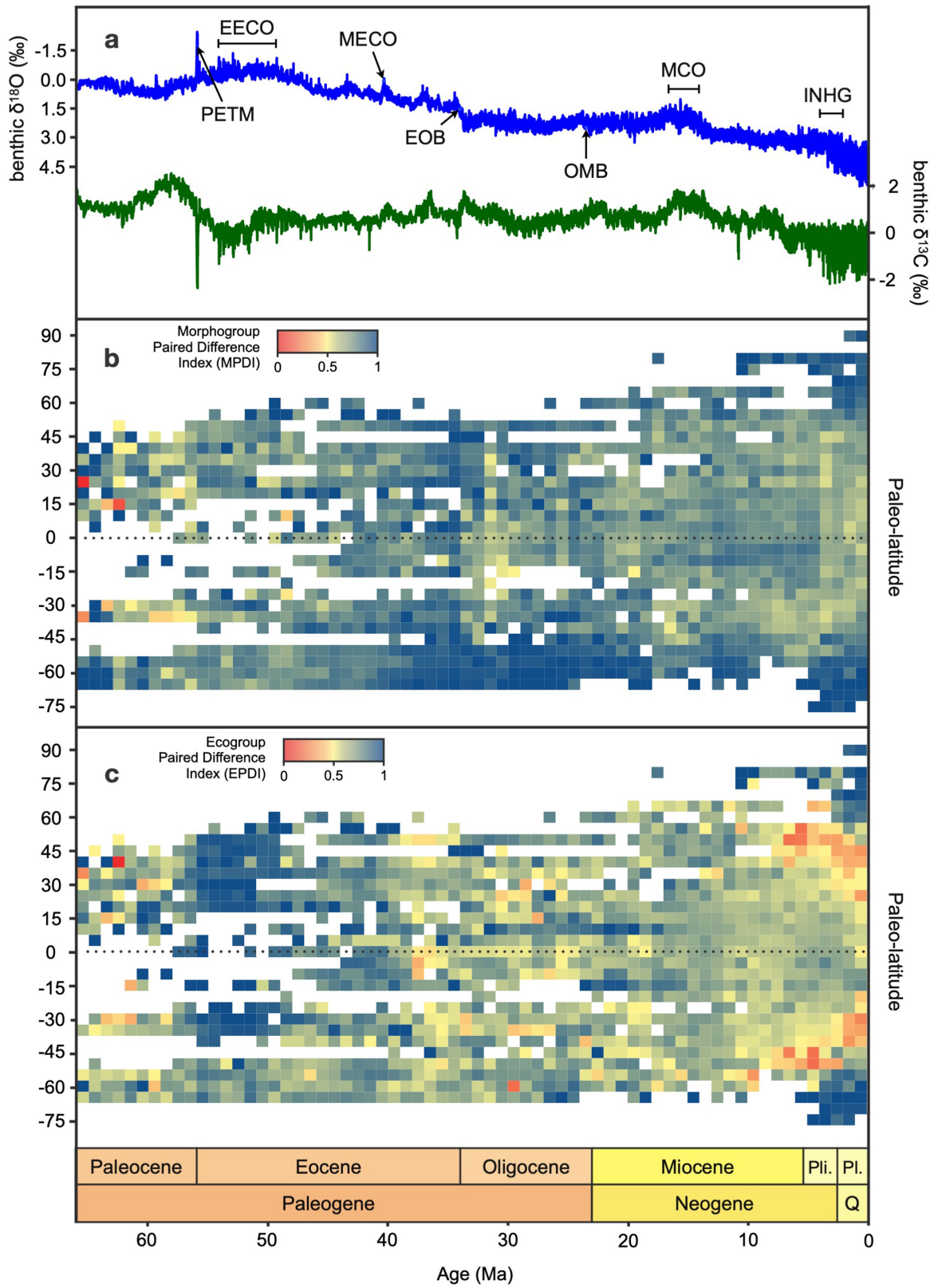

Extended Data Fig. 3 | Cenozoic climate and major climatic events, and specialization indices. (A) Benthic δ18O and δ13C from Westerhold et al.[19], PETM = Paleocene-Eocene Thermal Maximum, EECO = Early Eocene Climatic Optimum, MECO = Middle Eocene Climatic Optimum, EOT = Eocene-Oligocene Transition, OMB = Oligocene-Miocene Boundary, MCO = Miocene Climatic Optimum, INHG = Intensification of Northern Hemisphere Glaciation. (B) Morphogroup Paired difference index (MPDI), (C) Ecogroup Paired difference index (EPDI). Note that blue colors equal high ecogroup richness (B) or specialization (C), whereas red colors correspond to low values of each metric.

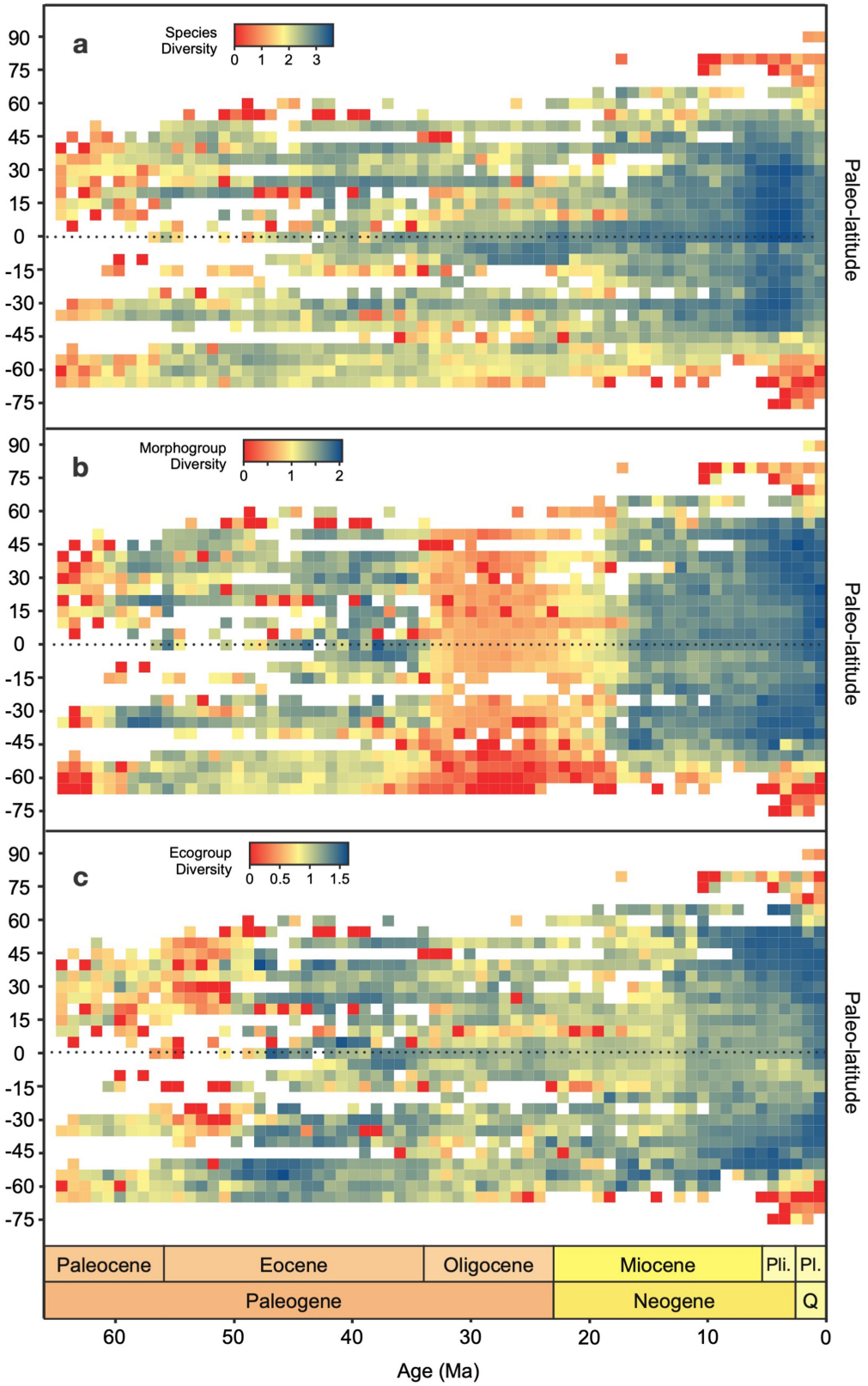

Extended Data Fig. 4 | Shannon diversity of species, morphogroups, and ecogroups during the Cenozoic. These metrics were calculated using Shannon entropy of count of each species (in A), morphogroup (in B) or ecogroup (in C) using the vegan package in R. Note that blue colors equal high ecogroup richness (B) or specialization (C), whereas red colors correspond to low values of each metric.

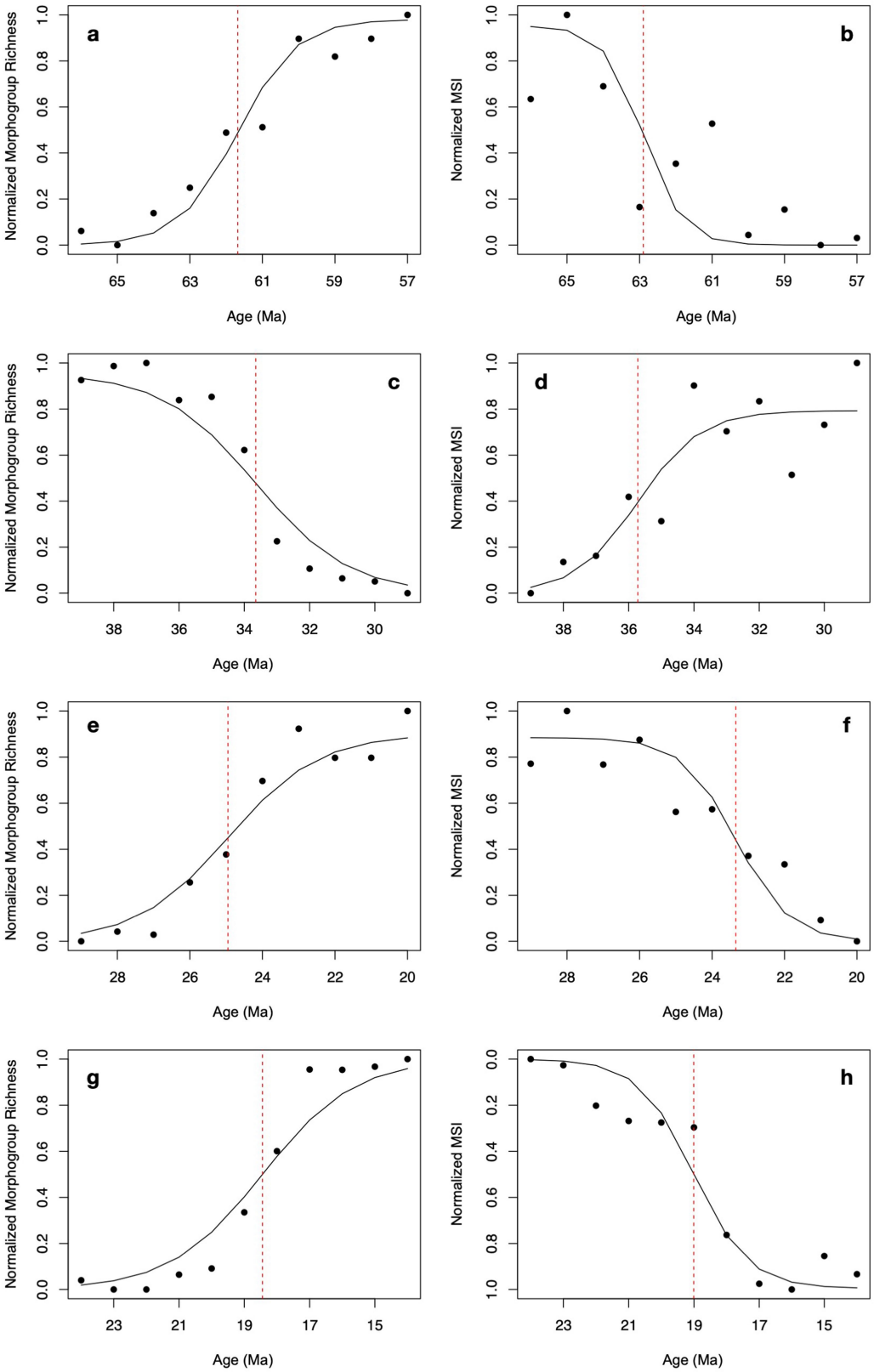

Extended Data Fig. 5 | Inflection points. Logistic function fitted to max-min normalized Morphogroup richness in (A) 66-57 Ma (Residual Standard Error (RSE): 0.07666), (C) 39-29 Ma (RSE: 0.04937), (E) 29-20 Ma (RSE: 0.07999) and (G) 24-14 Ma (RSE: 0.03875) and for max-min normalized Morphogroup Specialization Index (MSI)in (B) 66-57 Ma (RSE: 0.2119), (D) 39-29 Ma (RSE: 0.1722), (F) 29-20 Ma (RSE: 0.1036) and (H) 24-14 Ma (RSE: 0.1191) along with a line joining the predicted points from the logistic fit. The red dotted lines represent the point of inflection in each plot. Low values of RSE in these fits denote good fits.

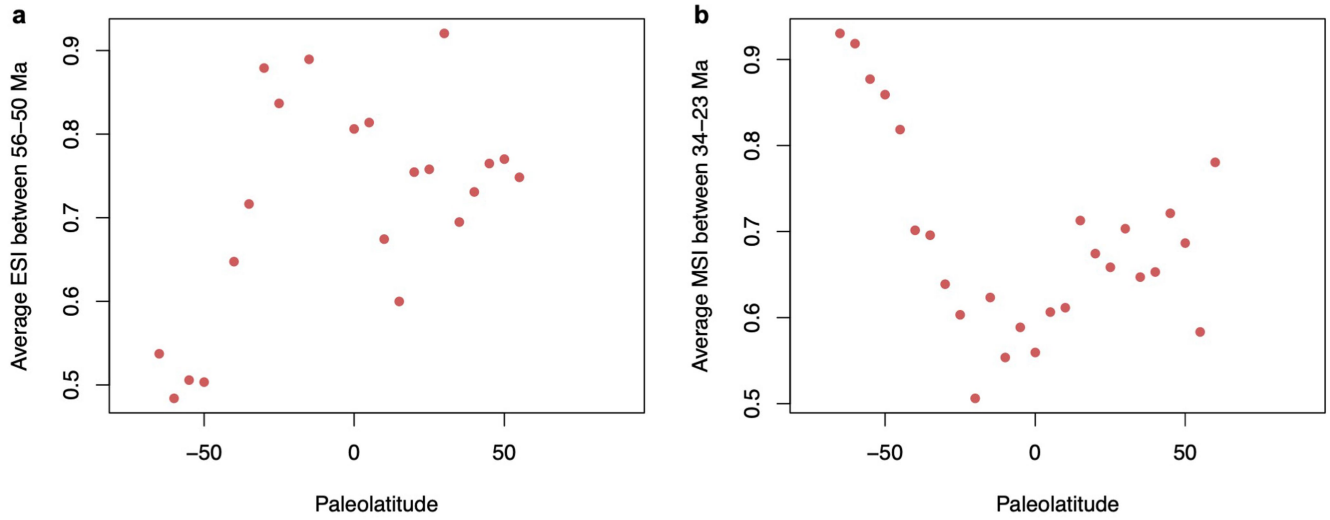

Extended Data Fig. 6 | Spatially averaged functional specialization across important time periods. (A) Average ESI between 56-50 Ma, (B) Average MSI between 34-23 Ma.

nature portfolio

Corresponding author(s): Anshuman Swain

Last updated by author(s): Feb 29, 2024

Reporting Summary

Nature Portfolio wishes to improve the reproducibility of the work that we publish. This form provides structure for consistency and transparency in reporting. For further information on Nature Portfolio policies, see our Editorial Policies and the Editorial Policy Checklist.

Statistics

For all statistical analyses, confirm that the following items are present in the figure legend, table legend, main text, or Methods section.

n/a	Confirmed	
☐	☒	The exact sample size (*n*) for each experimental group/condition, given as a discrete number and unit of measurement
☐	☒	A statement on whether measurements were taken from distinct samples or whether the same sample was measured repeatedly
☐	☒	The statistical test(s) used AND whether they are one- or two-sided *Only common tests should be described solely by name; describe more complex techniques in the Methods section.*
☐	☒	A description of all covariates tested
☐	☒	A description of any assumptions or corrections, such as tests of normality and adjustment for multiple comparisons
☐	☒	A full description of the statistical parameters including central tendency (e.g. means) or other basic estimates (e.g. regression coefficient) AND variation (e.g. standard deviation) or associated estimates of uncertainty (e.g. confidence intervals)
☐	☒	For null hypothesis testing, the test statistic (e.g. *F*, *t*, *r*) with confidence intervals, effect sizes, degrees of freedom and *P* value noted *Give P values as exact values whenever suitable.*
☒	☐	For Bayesian analysis, information on the choice of priors and Markov chain Monte Carlo settings
☒	☐	For hierarchical and complex designs, identification of the appropriate level for tests and full reporting of outcomes
☒	☐	Estimates of effect sizes (e.g. Cohen's *d*, Pearson's *r*), indicating how they were calculated

Our web collection on statistics for biologists contains articles on many of the points above.

Software and code

Policy information about availability of computer code

Data collection	No software was used for data collection. All data used in this project are available from the Triton dataset [Fenton & Woodhouse et al., 2021] (https://doi.org/10.1038/s41597-021-00942-7)
Data analysis	All analyses were performed using R Studio 2023.06.0+421 and R v4.2.2. All R packages (bipartite v2.19, iNEXT v3.0.0, vegan v2.6-4) used in the study are cited in the manuscript and in the code at https://doi.org/10.5281/zenodo.7888565

For manuscripts utilizing custom algorithms or software that are central to the research but not yet described in published literature, software must be made available to editors and reviewers. We strongly encourage code deposition in a community repository (e.g. GitHub). See the Nature Portfolio guidelines for submitting code & software for further information.

Data

Policy information about availability of data

All manuscripts must include a data availability statement. This statement should provide the following information, where applicable:

- Accession codes, unique identifiers, or web links for publicly available datasets
- A description of any restrictions on data availability
- For clinical datasets or third party data, please ensure that the statement adheres to our policy

All data used in this project are available from the Triton dataset [Fenton & Woodhouse et al., 2021] (https://doi.org/10.1038/s41597-021-00942-7)

Research involving human participants, their data, or biological material

Policy information about studies with human participants or human data. See also policy information about sex, gender (identity/presentation), and sexual orientation and race, ethnicity and racism.

Reporting on sex and gender	N/A
Reporting on race, ethnicity, or other socially relevant groupings	N/A
Population characteristics	N/A
Recruitment	N/A
Ethics oversight	N/A

Note that full information on the approval of the study protocol must also be provided in the manuscript.

Field-specific reporting

Please select the one below that is the best fit for your research. If you are not sure, read the appropriate sections before making your selection.

☐ Life sciences ☐ Behavioural & social sciences ☒ Ecological, evolutionary & environmental sciences

For a reference copy of the document with all sections, see nature.com/documents/nr-reporting-summary-flat.pdf

Ecological, evolutionary & environmental sciences study design

All studies must disclose on these points even when the disclosure is negative.

Study description	We work with planktonic foraminiferal species occurrences within samples, and use a network-based method and other statistical modeling to explore the spatio-temporal patterns in the data, with a focus on ecology and morphology.
Research sample	The research sample is sourced from the Triton dataset (Fenton & Woodhouse et al. 2021). This dataset contains planktonic foraminiferal occurrences through the last 66 million years, and due to the high preservation potential and taxonomic completeness of this organism record, they are the best fossil group available to perform global analyses of the scale presented.
Sampling strategy	The data is originally from Fenton & Woodhouse et al. (2021). The data was sampled at resolution of 1 Ma.
Data collection	Data was extracted from from the Triton dataset (Fenton & Woodhouse et al. 2021).
Timing and spatial scale	Start date: 66 Ma; end date: 0 Ma; sampling resolution: 1 Ma. Latitudinal bins of 5 degrees throughout this interval.
Data exclusions	We used the Triton dataset from 66-0 Ma, excluding all planktonic foraminiferal occurrences for species exhibiting microperforate and medioperforate wall textures as these species have a less well-refined phylogeny compared to macroperforate species (Pearson, 2018). All macroperforate planktonic foraminiferal species were assigned speciation and extinction datums in accordance with Aze et al. (2011) and Fenton & Woodhouse et al. (2021), and all species occurrences located outside of the assigned stratigraphic ranges were removed to eliminate much of the occurrence data likely attributable to misidentification and/or reworking.
Reproducibility	All code and data is available in public domain. Data is from Fenton & Woodhouse et al. (2021) and code is on https://doi.org/10.5281/zenodo.7888565
Randomization	Planktonic foraminifera were grouped into the ecogroups and morphogroups of Aze et al. (2011), to test the primary hypotheses.
Blinding	Blinding is not applicable as we were working with aggregate data and occurrences of species.

Did the study involve field work? ☐ Yes ☒ No

Reporting for specific materials, systems and methods

We require information from authors about some types of materials, experimental systems and methods used in many studies. Here, indicate whether each material, system or method listed is relevant to your study. If you are not sure if a list item applies to your research, read the appropriate section before selecting a response.

Materials & experimental systems

n/a	Involved in the study
☒	☐ Antibodies
☒	☐ Eukaryotic cell lines
☐	☒ Palaeontology and archaeology
☒	☐ Animals and other organisms
☒	☐ Clinical data
☒	☐ Dual use research of concern
☒	☐ Plants

Methods

n/a	Involved in the study
☒	☐ ChIP-seq
☒	☐ Flow cytometry
☒	☐ MRI-based neuroimaging

Palaeontology and Archaeology

Specimen provenance	The Triton dataset (Fenton & Woodhouse et al. 2021)
Specimen deposition	See the Triton dataset (Fenton & Woodhouse et al. 2021)
Dating methods	No new dates provided.

☒ Tick this box to confirm that the raw and calibrated dates are available in the paper or in Supplementary Information.

Ethics oversight	No ethical approval or guidance was required, as the data was already collected/collated in Fenton & Woodhouse et al. (2021)

Note that full information on the approval of the study protocol must also be provided in the manuscript.

Plants

Seed stocks	N/A
Novel plant genotypes	N/A
Authentication	N/A